the FEBS Journal

Bifunctional ADP-dependent phosphofructokinase/glucokinase activity in the order *Methanococcales* – biochemical characterization of the mesophilic enzyme from *Methanococcus maripaludis*

Victor Castro-Fernandez, Felipe Bravo-Moraga, Alejandra Herrera-Morande and Victoria Guixe

Departamento de Biología, Facultad de Ciencias, Universidad de Chile, Santiago, Chile

Keywords
ADP-dependent sugar kinases; bifunctional enzyme; glucokinase; gluconeogenesis; phosphofructokinase

Correspondence
V. Guixe, Departamento de Biología, Facultad de Ciencias, Universidad de Chile, Las Palmeras 3425, Ñuñoa, Santiago, Chile, 7800003.
Fax: +56 2 227 12983
Tel: +56 2 297 87335
E-mail: vguixe@uchile.cl

(Received 26 September 2013, revised 23 January 2014, accepted 17 February 2014)

doi:10.1111/febs.12757

In some archaea, the phosphorylation of glucose and fructose 6-phosphate (fructose 6*P*) is carried out by enzymes that are specific for either substrate and that use ADP as phosphoryl donor. In the hyperthermophilic archaeon *Methanocaldococcus jannaschii*, a bifunctional enzyme able to phosphorylate glucose and fructose 6*P* has been described. To determine whether the ability to phosphorylate both glucose and fructose 6*P* is a common feature for all enzymes of the order *Methanococcales*, we expressed, purified and characterized the unique homologous protein of the mesophilic archaea *Methanococcus maripaludis*. Assay of the enzyme activity with different sugars, metals and nucleotides allows us to conclude that the enzyme is able to phosphorylate both fructose 6*P* and glucose in the presence of ADP and a divalent metal cation. Kinetic characterization of the enzyme revealed complex regulation by the free Mg^{2+} concentration and AMP, with the latter appearing to be a key metabolite. To determine whether this enzyme could have a role in gluconeogenesis, we evaluated the reversibility of both reactions and found that glucokinase activity is reversible, whereas phosphofructokinase activity is not. To determine the important residues for glucose and fructose 6*P* binding, we modeled the bifunctional phosphofructokinase/glucokinase enzyme from *M. maripaludis* and its interactions with both sugar substrates using protein–ligand docking. Comparison of the active site of the phosphofructokinase/glucokinase enzyme from *M. maripaludis* with the structural models constructed for all the homology sequences present in the order *Methanococcales* shows that all of the ADP-dependent kinases from this order would be able to phosphorylate glucose and fructose 6*P*, which rules out the current annotation of these enzymes as specific phosphofructokinases.

Database
Model data are available in the Protein Model Data Base under accession numbers PM0079106, PM0079107, PM0079108, PM0079109, PM0079110, PM0079111, PM0079112, PM0079113, PM0079114, PM0079115 and PM0079116

Abbreviations
EM, Embden–Meyerhof; fructose 1,6-bis*P*, fructose 1,6-bisphosphate; fructose 6*P*, fructose 6-phosphate; GK, glucokinase; glucose 6*P*, glucose 6-phosphate; MmPFK/GK, bifunctional phosphofructokinase/glucokinase enzyme from *Methanococcus maripaludis*; PFK, phosphofructokinase.

Introduction

The archaea domain presents modifications of the classical Embden–Meyerhof (EM) pathway. One of the most striking modifications present in some genera of Euryarchaeota is the phosphorylation of glucose and fructose *6*-phosphate (fructose 6*P*) by ADP as a phosphoryl donor, instead of ATP, as in the classical pathway. These ADP-dependent sugar kinases are able to phosphorylate glucose (ADP-GKS; EC 2.7.1.147) or fructose 6*P* (ADP-PFK; EC 2.7.1.146) and are homologous between them, although they show no sequence similarity to any ATP-dependent kinase known to date. For this reason, these proteins were proposed as a new family of enzymes [1], and subsequently were classified as belonging to the ribokinase superfamily, given the structural similarity with its members [2]. In the Euryarchaeota kingdom, ADP-dependent sugar kinases have been annotated in the orders: *Pyrococcus, Thermococcus, Methanosarcina, Methanosaeta, Methanococcoides, Methanococcus, Methanocaldococcus* and *Archaeoglobus* [3]. To date, the best characterized enzymes are from the *Thermococcales* group. Glucokinases (GK) from *Thermococcus litoralis* [4] and *Pyrococcus furiosus* [5] shown to be specific for glucose, as well as phosphofructokinases (PFK) from *Pyrococcus horikoshii* [6], *Thermococcus zilligii* [7], *Pyrococcus furiosus* [1] and *Archeaoglobus fulgidus* [8], are specific for fructose 6*P*. In the order *Methanococcales*, ADP-PFK activity has been detected in cellular extract from *Methanococcus jannaschii*, *Methanococcus (Methanotorris) igneus* and *Methanococcus maripaludis* [9]. Subsequently, the enzyme from the hyperthermophilic methanogenic archeon *Methanocaldococcus jannaschii* was described as a bifunctional enzyme able to phosphorylate glucose and fructose 6*P* [10]. Given its dual activity, this enzyme was initially proposed as an ancestral state for all the family, although a subsequent study showed that this enzyme is not an ancestral form [11]. However, the same study did not address whether this dual character is a particular feature of the *M. jannashii* enzyme or whether it is a common feature for all the enzymes of the order *Methanococcales*. Moreover, in the genome of the mesophilic archaea *M. maripaludis*, there is a unique ADP-dependent homologous protein, which raises the question of whether this homologous has both GK and phosphofructokinase activities.

Recently, a bifunctional fructose 1,6-bisphosphate-aldolase/phosphatase virtually present in all archaeal groups, as well as the deeply branching bacterial lineages, has been reported [12]. It was proposed that this enzyme ensures unidirectional gluconeogenesis under conditions where the carbon flux does not need to be turned to sugar degradation. Based on its phylogeny and distribution pattern, Say and Fuchs [13] proposed that the bifunctional fructose 1,6-bisphosphatealdolase/phosphatase represents the ancestral gluconeogenic enzyme, supporting an evolutionary scenario where gluconeogenesis preceded glycolysis. On the other hand, the autotrophic methanogens such as *M. maripaludis* grow on a limited range of substrates, including acetate, molecular hydrogen, compounds of 1C such as methylamines and formate, and few alcohols [14]. They are able to store glycogen, but not assimilated sugars, indicating that, besides participating in glycolysis, ADP-dependent kinases could also have a role in glucose synthesis, although this issue has not been evaluated. Anabolism and catabolism of glycogen is of evolutionary interest for comparison with heterotrophic archaea, as well as with respect to the potential applications of these methanogenic organisms in biotechnology.

In the present study, we addressed the expression, purification and biochemical characterization of the unique ADP-dependent homologous protein present in the genome of the mesophilic archaea *M. maripaludis*. Our results demonstrate that this enzyme is bifunctional capable of phosphorylating both glucose and fructose 6*P* (MmPFK/GK). Considering that less developed organisms, such as those from the order *Methanococales*, lack the ability to assimilate glucose but are able to store glycogen, the reversibility of the MmPFK/GK glucokinase (GK) activity supports the fact that this enzyme could have a role in glucose synthesis. Characterization of the enzyme revealed a complex regulation by the free Mg^{2+} concentration and AMP, with the latter appearing to be a key metabolite. On the other hand, molecular modeling of the MmPFK/GK enzyme along with protein–ligand docking with both substrates allows us to determine residues important for substrate binding. Finally, molecular models constructed for all ADP-dependent kinases from the order *Methanococcales* indicate that all of these enzymes would be bifunctional, and thus able to phosphorylate glucose and fructose 6*P*.

Results and Discussion

Phylogenetic tree

To analyze the evolutional history of the ADP-dependent sugar kinases from the order *Methanococcales*, we inferred a phylogenetic tree with the available sequences from the nonredundant protein database. Characterized homologous PFK enzymes sequences from *Thermococcales* were used as an outgroup to root

the tree (Fig. 1). The tree obtained for the *Methanococcales* group was similar to the one obtained for the complete family [15]. Our inferred tree contains 11 sequences from the order *Methanococcales*; among them are sequences from thermophilic organisms of the *Methanocaldococcaceae* family (genus *Methanocaldococcus* and *Methanotorris*) and the *Methanoccocacea* family (genus *Methanothermococcus*), as well as mesophilic organisms from the genus *Methanococcus* of this latter family.

In the *Methanococcales* group, the enzyme from *M. jannaschii* is the only ADP-dependent sugar kinase characterized that is capable of using glucose and fructose 6*P* as phosphoryl acceptor substrate. According to the information available in the *Kyoto Encyclopedia of Genes and Genomes* (http://www.genome.ad.jp/kegg/), the genome of this organism has only one homologous gene; accordingly, it has been proposed that this enzyme would act as a bifunctional phosphofructokinase/GK enzyme *in vivo* [10]. By contrast, the genome of the *Thermococcales* group has two copies of this gene and presents separate phosphofructokinase and GK activities. To determine whether the phosphorylation of glucose and fructose 6*P* is carried out exclusively by enzymes of the ADP-dependent sugar kinases family in the modified EM pathway of the orders *Thermococcales* and *Methanococcales*, we searched for ATP dependent hexokinases and phosphofructokinases homologous genes in the *Kyoto Encyclopedia of Genes and Genomes* database. We found no counterpart of these genes; thus, in the *Thermococcales* group, glucose and fructose 6*P* phosphorylation is carried out only by specific enzymes of the ADP-dependent sugar kinases family, whereas, in the *Methanococcales* group, both reactions would be carried out by the same enzyme encoded by a unique gene.

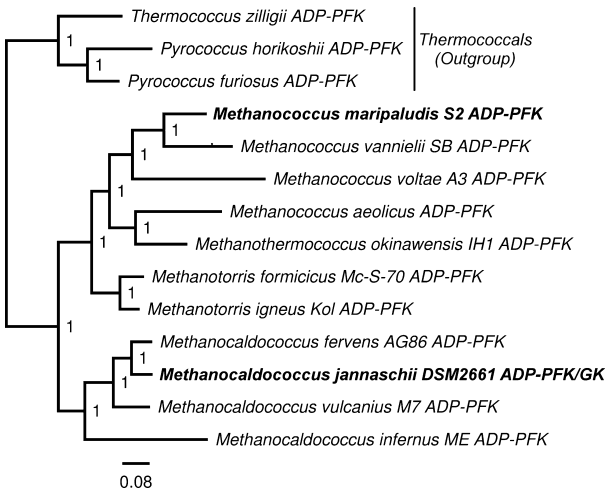

Fig. 1. Phylogenetic tree of ADP-dependent sugar kinases from the order *Methanococcales*. PFK sequences from the order *Thermococcales* were used as an outgroup. The posterior probability of each node is shown in each split. The position of the *M. jannaschii* and *M. maripaludis* sequences is highlighted in bold.

Biochemical characterization of the enzyme from *M. maripaludis*

The optimized synthetic gene of the ADP-dependent enzyme from *M. maripaludis* strain S2 (UniProt Protein Database Code: Q6LXQ3) was expressed in *Escherichia coli*. The protein was purified and analyzed by SDS/PAGE (Fig. S1). Analysis of its oligomerization state by gel exclusion chromatography revealed that the enzyme is a monomer, which is usually the oligomeric state found for other proteins of the family, including the *M. jannaschii* enzyme [10].

To analyze the sugar substrate ambiguity of this enzyme, we evaluated 16 different sugars as a phosphoryl acceptor (Fig. 2A). Among these, only glucose and fructose 6*P* showed ADP consumption. None of the other sugars tested demonstrated a significant consumption of the nucleotide relative to the control without sugar. These results indicate that the mesophilic *M. maripaludis* enzyme is not promiscuous in terms of sugar substrate specificity but, instead, is specific for glucose and fructose 6*P*. At a sugar concentration of 10 mM, the MmPFK/GK enzyme showed higher activity with glucose compared to that obtained with fructose 6*P*; with this latter substrate having 75% of the activity measured with glucose.

To confirm that this enzyme is a true ADP-dependent kinase, we assayed the enzyme activity in the presence of several nucleotides, using glucose or fructose 6*P* as a sugar substrate. The highest activity was obtained in the presence of ADP, although phosphoryl group transfer from other diphosphorylated nucleotides was observed, albeit at a significantly slower rate (Fig. 2B). In the presence of ATP, no activity was detected.

Divalent cations were required for MmPFK/GK activity. Among the divalent metal cations tested, the highest activity was observed in the presence of Mg^{2+}, although, in the presence of Co^{2+}, Ni^{2+} and Mn^{2+}, significant activity was also measured (Fig. 2C). The presence of EDTA in the reaction mixture completely abolished enzyme activity, indicating that the metal–nucleotide complex is the true substrate for the enzyme reaction.

When investigating the pH at which maximum activity is obtained, we found maximum PFK activity at pH 6.5, whereas GK maximal activity was found at

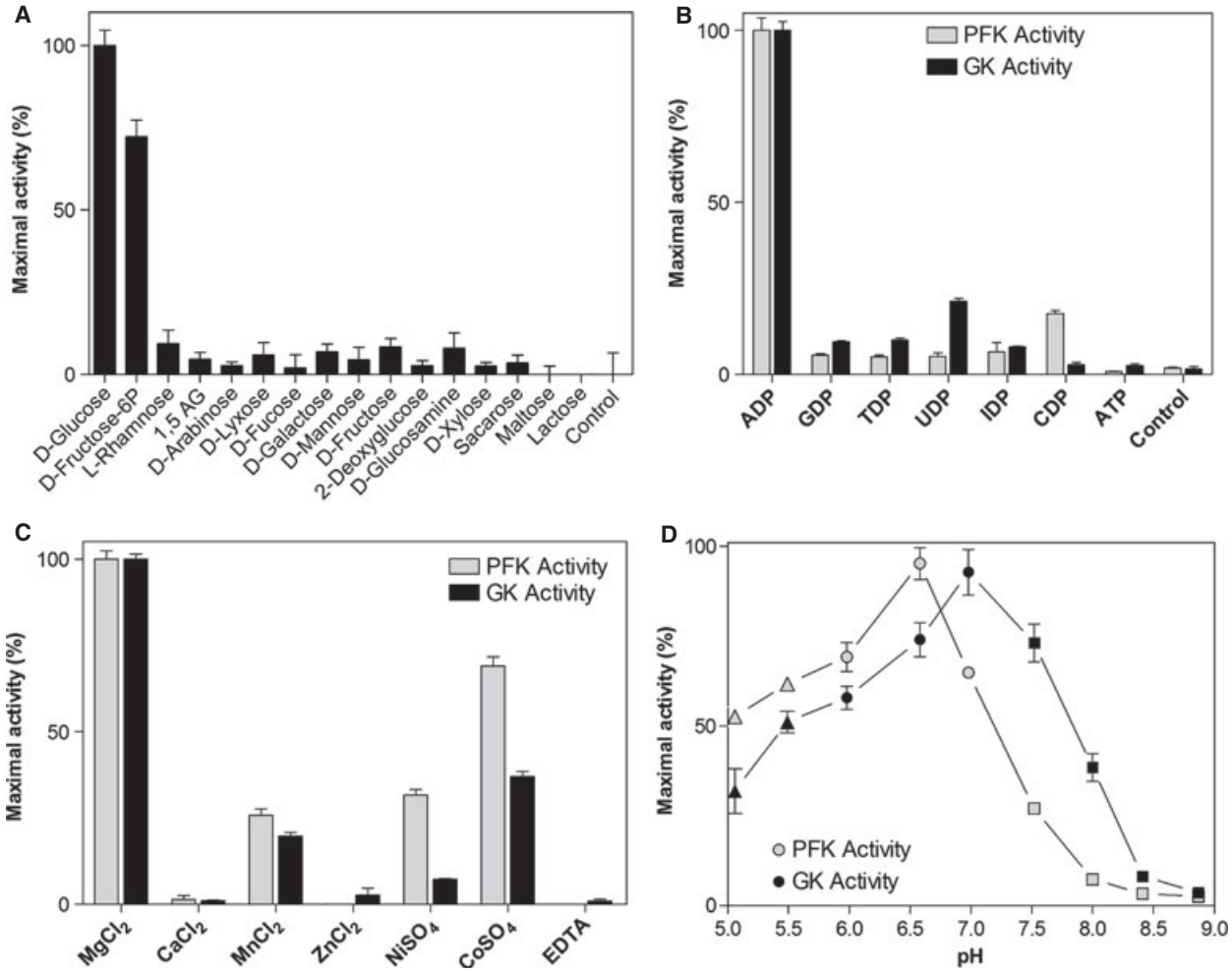

Fig. 2. Biochemical characterization of MmPFK/GK. (A) ADP-dependent kinase activity measured as ADP consumption with different sugar substrates (10 mM). Activity is shown as the percentage of activity measured in the presence of glucose. 1,5 AG, 1,5-anhidroglucitol. Control corresponds to activity in the absence of sugar. (B) GK and PFK activity with different nucleotides as a phosphoryl donor. (C) GK and PFK activity in the presence of 1 mM ADP, 2 mM of a different divalent cation and 1 mM glucose or fructose 6*P*. EDTA 50 mM was used as a control without metal. (D) GK and PFK activity at different pH values; pH 5.0 and 5.5 for acetate/acetic acid; pH 6.0, 6.6 and 7.0 for Pipes/NaOH; pH 7.5, 8.0, 8.5 and 8.9 for Tris-HCl.

pH 7.0 (Fig. 2D). The lower optimum pH obtained in the case of the ADP-PFK activity has been associated with the protonation of a lysine group involved in stabilization of the phosphate group of fructose 6*P* [11].

Kinetic characterization of the MmPFK/GK enzyme

To evaluate the specificity of the MmPFK/GK enzyme with respect to glucose or fructose 6*P*, we determined the kinetic parameters performed for both sugars in the presence of Mg-ADP (Fig. S2). The activity using fructose 6*P* as substrate shows hyperbolic behavior, whereas the saturation curve for glucose exhibits substrate inhibition at high glucose concentrations (> 200 mM). On the other hand, the saturation curves for both PFK and GK activity with Mg-ADP as substrate showed substrate inhibition (Fig. S2). Table 1 shows the kinetic parameters obtained from nonlinear adjustments of the saturation curves. The k_{cat}/K_m values are 2.53×10^5 and 5.7×10^2 $M^{-1} \cdot s^{-1}$ for fructose 6*P* and glucose, respectively. These results show that, when two competing substrates such as these were present in an equimolar mixture, the rate at which fructose 6*P* is phosphorylated is 440-fold higher than the glucose phosphorylation rate. This difference in the value of the k_{cat}/K_m parameter is mainly a result of the dissimilar values of K_m for both substrates. The K_m for

Table 1. Kinetic parameters of MmPFK/GK.

Sugar	K_m (mM)	k_{cat} (s^{-1})	k_{cat}/K_m ($M^{-1}.s^{-1}$)	K_i (mM)
Direct reaction				
Glucose	40 ± 5	23 ± 1	5.75×10^2	895 ± 205
Fructose 6*P*	0.065 ± 0.014	16.5 ± 0.6	2.53×10^5	–
MgADP (GK)	16 ± 6	48 ± 12	3.00×10^3	25 ± 10
MgADP (PFK)	8 ± 2	30 ± 4	3.75×10^3	54 ± 21
Reverse reaction				
Glucose 6P	0.623 ± 0.076	0.678 ± 0.015	1.09×10^3	–
Fructose 1,6-Bis*P*	0.120 ± 0.016	0.45 ± 0.02	3.75×10^3	–

fructose 6*P* is in the micromolar range, whereas, for glucose, a K_m of 40 mM was obtained. Although the enzyme from *M. jannaschii* is also more specific for fructose 6*P*, its k_{cat}/K_m ratio is only 60-fold greater for this substrate compared to the value obtained for glucose [10]. Interestingly, despite its high K_m for glucose, the activity of the MmPFK/GK enzyme with this substrate is higher compared to other sugars, which is mainly a result of its high k_{cat} value. Noticeably, the K_m values for ADP in the GK and PFK reactions (16 and 8 mM, respectively) are much higher than those reported for the *M. jannaschii* enzyme (0.032 and 0.63 mM, respectively). Because regulation of the enzyme activity by divalent metal cation has been reported previously [16], we determined the effect of the free Mg^{2+} concentration on the kinetic parameters. Indeed, in the presence of the 1 mM free Mg^{2+} concentration (instead of the 5 mM Mg^{2+} in excess over the nucleotide concentration used in the experiments shown in Table 1), the K_m values for Mg-ADP in the GK and PFK reaction diminished dramatically, reaching values of 0.3 and 1.2 mM, respectively. A similar scenario is also observed for several enzymes of the ribokinase superfamily whose activity is strongly dependent on the amount of free divalent metal cation present. In some members, this second metal, in addition to the one present in the metal nucleotide complex, acts by inhibiting enzyme activity, whereas, in others, it acts as an activator. In a previous study, we investigated the regulation of specific ADP-dependent GK and PFK enzymes from *Thermococcales* by divalent metal cations and found that only GKs are inhibited in a significant degree by the free metal. For these enzymes, the K_m values for the metal–nucleotide complex are not significantly affected by the concentration of free metal and so a mechanism was proposed where the binding of a second metal produces a complex with a reduced catalytic constant [16]. However, in the MmPFK/GK enzyme, a different situation is observed; the free Mg^{2+} concentration has a profound effect on the K_m values for MgADP in the GK and PFK reactions, whereas it has no significant effect on the V_{max} of both reactions. Although the data suggest a competitive inhibition of free Mg^{2+} (binding of free metal and MgADP substrate to the same enzyme form), a detailed inhibition mechanism requires additional knowledge of the general kinetic mechanism of the GK and PFK reactions and the dissociation constants for Mg^{2+} binding, amongst other data. On the other hand, although the intracellular Mg^{2+} concentration in these organisms is not known, even at a concentration of approximately 5 mM of the free cation, the enzyme exhibits significant activity at glucose concentrations between 5 and 10 mM, mainly as a result of its high k_{cat}. This implies that this activity would be relevant for the *in vivo* function and that the enzyme could be performing both GK and PFK functions *in vivo*.

Although the MmPFK/GK enzyme is unable to use other substrate besides glucose and fructose 6*P* as substrates, we aimed to further assess the binding specificity by evaluating the ability of the enzyme to accommodate other sugars at the active site. Accordingly, we assayed the ability of different sugar to inhibit the GK and PFK reactions. We employed a set of 14 sugars, besides glucose and fructose 6*P*, at a fixed concentration of 10 mM for each. For the PFK reaction, none of the sugars tested were able to inhibit the activity significantly (Fig. 3A) with the only exception of glucose, which inhibits enzyme activity by approximately 20%, as would be expected if both sugar substrates bind to the same active site. For the GK reaction, the results are almost the same, except for glucosamine, which results in approximately 40% activation (Fig. 3B). The activation effect is concentration dependent and is not an artefact of the assay (data not shown). In this case, strong inhibition of the GK reaction was observed in the presence of fructose 6*P*, which can be explained by the low K_m of the enzyme for the phosphorylated sugar, which is present at a concentration of 10 mM, as well as by the high K_m for glucose measured under this experimental condition (approximately 5 mM free Mg^{2+}). A more detailed inspection of the inhibitory range of both sugars allowed us to determine an IC_{50} value of 220 μM for

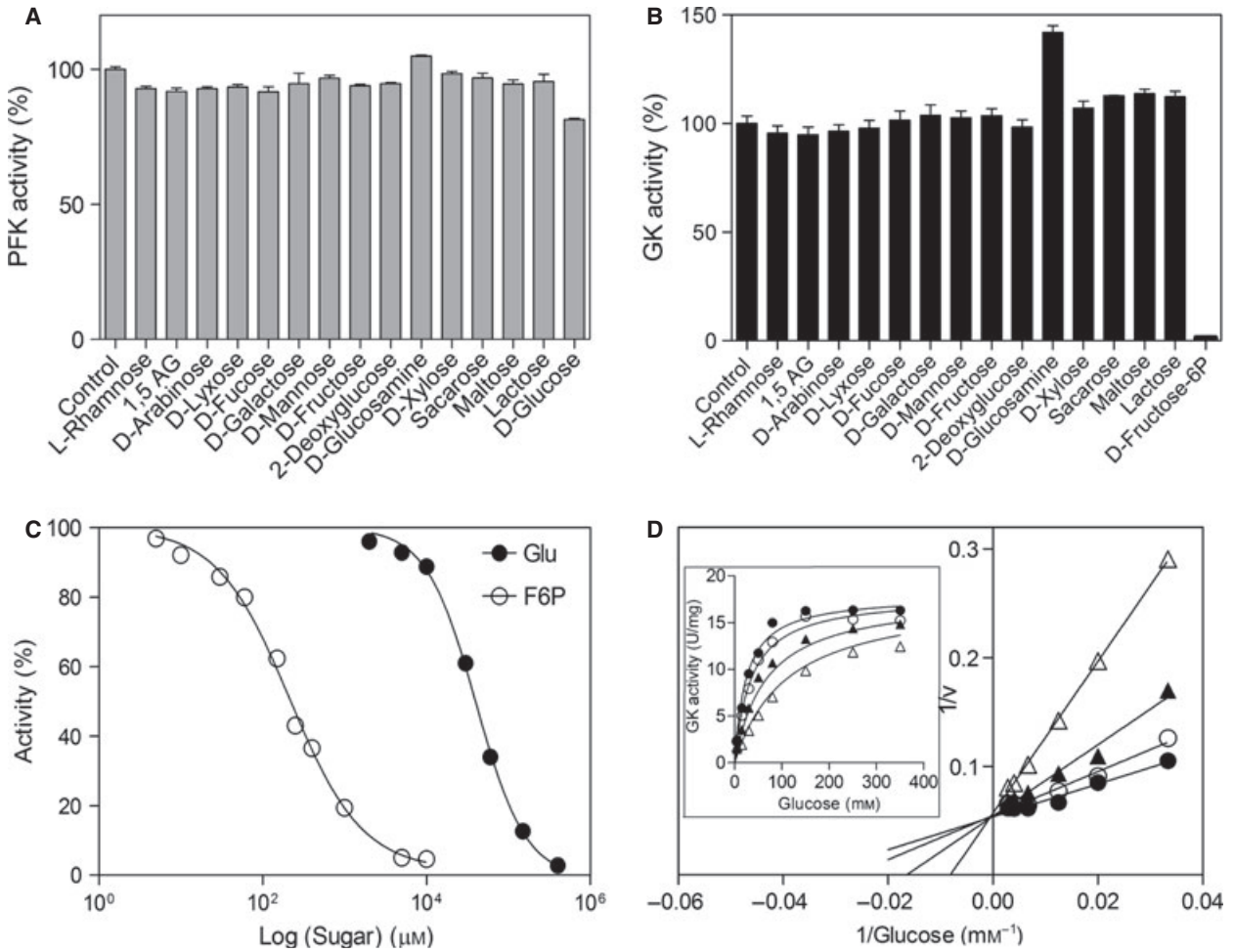

Fig. 3. Inhibition of MmPFK/GK by sugars. (A) Inhibition of PFK activity by different sugars at 10 mM, activity without inhibitor was used as a control, 1,5 AG, 1,5-anhidroglucytol. Only glucose presented significant inhibition (20% of inhibition). (B) Inhibition of GK activity by different sugars at 10 mM; in the presence of fructose 6*P*, only 2% of residual activity was detected. Interestingly, in the presence of glucosamine, 40% activation was observed. (C) Dose–response inhibition of GK activity (white circles) by fructose 6*P* (F6P) and inhibition of PFK activity (black circles) by glucose (Glu). The IC_{50} for fructose 6*P* and glucose was 220 μM and 40 mM, respectively. (D) Double-reciprocal plot for competitive inhibition of GK activity by fructose 6*P*. Fructose 6*P* concentrations were: 0 mM (black circles), 0.1 mM (white circles), 0.4 mM (black triangles) and 0.8 mM (white triangles). Inset: global fit to a competitive inhibition mechanism, a K_i of 226 μM for fructose 6*P* was determined. Error bars in (A) and (B) indicate the SE of three independent measurements.

fructose 6*P* in the GK reaction and an IC_{50} of 40 mM for glucose in the PFK reaction (Fig. 3C). Binding of both substrates to the same active site was demonstrated by the competitive inhibition of fructose 6*P* when glucose was used as the variable substrate (Fig. 3D), where a K_i value of 226 μM was obtained.

Molecular modeling of MmPFK/GK

To study the structural determinants of the sugar specificity, the structure of the ADP-dependent PFK/GK from *M. maripaludis* was modeled using homology modeling (Table S1). With this model, we performed docking assays with fructose 6*P* and glucose, and then the Mg-ADP complex was mounted onto the resulting docking structures. The whole structures were subjected to an energy minimization process (Fig. 4A). For ADP, inspection of residues present within 5 Å away from the nucleotide identified: K76, P77, Q105, K175, E176, Q191, S192, N193, R194, I196, E270, D297, E298, E300, H345, T346, M347, Y348, I350, A376, S377, A380, S429, R430, I431, V432, E433, N434, P435, T438, G440, L441, G442, D443, T444 and I445. Among these M347, I431 and L441 create a hydrophobic pocket around the adenine group; R194 makes a hydrogen bond with α and β phosphates; carbonyl and NH groups from V432 peptide bond make a hydrogen bond with tye NH_2 group of C6 and the

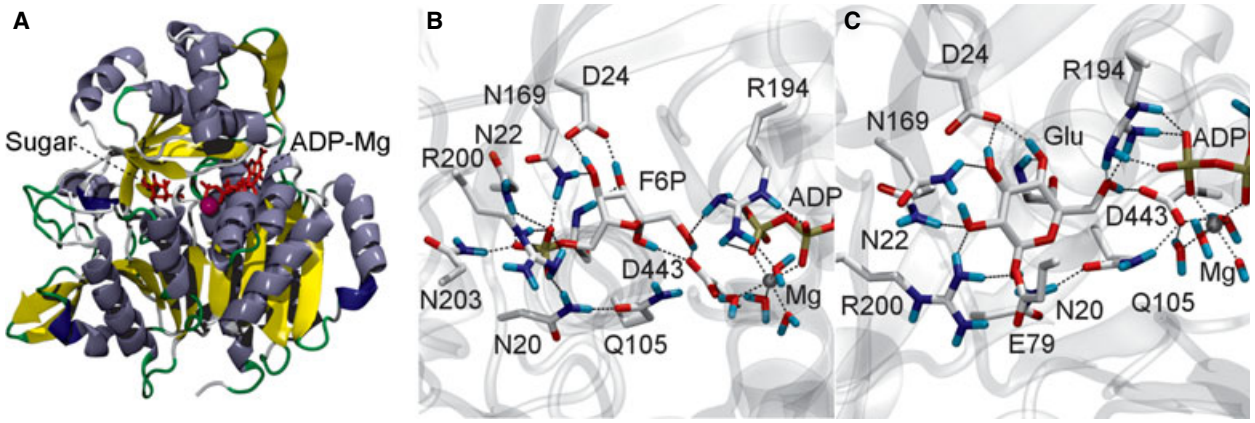

Fig. 4. Protein–ligand interaction modeling results. (A) Homology model of MmPFK/GK; sugar and nucleotide binding sites are indicated. Substrates are shown as red sticks and Mg^{2+} is shown as a magenta sphere. (B) β-D-fructose 6*P* docked in MmPFK/GK enzyme after the energy minimization procedure. (C) β-D-glucose docked in MmPFK/GK enzyme after the energy minimization procedure. Hydrogen bonds are shown as a dotted line in (B) and (C).

N1 atom of adenine; the carbonyl group from peptide bond of H345 makes hydrogen bonds with the C3 hydroxyl of the ribose ring and the NH groups from peptides bonds of G440 and L441; and G442 and D443 make hydrogen bonds with the β phosphate of ADP, whereas both phosphates (α and β) are coordinated to a Mg^{2+} ion. On the other hand, the waters that coordinate the Mg^{2+} ion interact with the carbonyl group of the peptide bond F271, as well as the side chains of E270, E300, H345 and D443 (Fig. S3). E270 and E300 corresponds to residues present in the HXE and NXXE motifs, respectively, which have been described as divalent cation binding sites in the ADP-dependent sugar kinases family [16].

For glucose, analysis of residues that have at least one atom within an area of 5 Å away from the sugar identified the residues; N20, N22, D24, E79, G103, G104, Q105, I108, N169, R170, I171, R194, I196, A198, R200, G230, Q232, A272, V439, G440 and D443. For fructose 6*P*, the residues were essentially the same, excluding E79, R170, I196, A198, Q232 and A272, and adding V21, K167 and N203.

The active site of MmPFK/GK modeled with fructose 6*P* (Fig. 4B) shows that the phosphate group of fructose 6*P* is stabilized by hydrogen bonds established through the side chains of residues N20, N22, N169, R200 and N203. On the other hand, D24 interacts with the hydroxyl groups of C3 and C4 of the furanose ring, whereas the NH group of the peptide bond of G104 interacts with the C3 hydroxyl, the N169 interacts with the C4 hydroxyl, the R194 interacts with the C1 hydroxyl and D443 interacts with the C1 and C2 hydroxyls (Fig. 4B). Residues R194 and D443 also interact with the C1 hydroxyl phosphoryl acceptor group. The catalytic mechanism of the ribokinase superfamily members is highly conserved, where an aspartic acid (or cysteine) acts as the catalytic base that subtracts the hydroxyl hydrogen, creating an alkoxide ion that is stabilized by an arginine (or lysine) residue, which in turns allows the nucleophilic attack to β (or γ) phosphate of the Mg-ADP (or Mg-ATP) substrate [3]. Site-directed mutagenesis of the aspartic residue in several members of ribokinase superfamily members provokes a dramatic loss of activity [3]. Also, site-directed mutagenesis of the positive residue noted above for the ADP-dependent PFK from *P. horikoshii* (R185) causes a dramatic decrease of activity [6]. In MmPFK/GK, these residues correspond to R194 and D443, which make appropriate interactions with the substrates with respect to their roles in the catalytic mechanism proposed for the whole superfamily.

Residue side chains involved in the stabilization of glucose through hydrogen bonds are N20 and E79 with the C1 hydroxyl group, as well as N22 with the C2 hydroxyl group, whereas R200 forms a hydrogen bond with the C1 and C2 hydroxyls groups; N169 forms a bond with the C2 and C3 hydroxyls groups; D24 forms a bond with the C3 and C4 hydroxyls groups; and the NH group from peptide bond of G104 forms a bond with the C4 hydroxyl. R194 and D443 established an interaction with the C6 hydroxyl group, which is the phosphate group acceptor (Fig. 4C). As in fructose 6*P*, R194 and D443 enable glucose to accommodate an appropriate orientation for catalysis. On the other hand, the results of molecular modeling show that both sugars are bound to the enzyme by essentially the same residues, except for N203, which established an interaction only when the

substrate was fructose 6*P*, and E79, which interacts only with glucose. However, analysis of the whole family sequences shows that E79 is present in specific GKs and also that N203 is conserved in all specifics GKs from *Methanosarcinales* and *Thermococcales* but is absent in PFKs from *Methanosarcinales* and *Thermococcales*. This suggests that the role of these residues in substrate specificity is unclear and that more thorough evolutionary studies are needed to demonstrate the contribution of these or other residues to substrate specificity in the whole family.

To determine whether active site glucose interactions are preserved throughout the order *Methanococcals*, we constructed homology models of all of the ADP-dependent sugar kinases available for this order (Table S2), except for the enzyme from *M. jannaschii*, which has already been studied *in vitro* [10] and *in silico* [11]. We performed a structural superposition of each of the nine models constructed in the presence of glucose with the one built for the *M. maripaludis* enzyme (Fig. S4). We found that residues present in a 5-Å cut-off area from glucose are completely conserved in the order *Methanococcales*, which supports the idea that all of the proteins of this order would be able to bind glucose besides fructose 6*P*, as was noted up to now.

Role of MmPFK/GK in glucose synthesis

Previous studies have proposed that the EM pathway has an gluconeogenic origin [7,13], which is consistent with the theory of an chemoautrophic origin of metabolism [17]. For example, less developed organisms, such as those from the order *Methanococcales*, lack the ability to assimilate glucose but are able to store glycogen [18]. Metabolic pathways in higher organisms operate through the degradation of organic compounds and CO_2 release, whereas most primitive organisms work as CO_2 fixers for compound formation [19]. Therefore, we investigated the possible role of the MmPFK/GK enzyme in glucose formation by analyzing its reverse catalysis for the PFK and GK activity. Unexpectedly, in contrast to that found for the direct reaction, the K_m for glucose 6-phosphate (glucose 6*P*) is 623 μM (Table 1) instead of the value of 40 mM determined for glucose. However, for the reverse reaction, the k_{cat} value is 34-fold lower than that obtained for the direct reaction. Analysis of the k_{cat}/K_m ratios shows that the glucose dephosphorylation reaction is two-fold more efficient than its phosphorylation. Even though this difference is marginal, it indicates that the MmPFK/GK enzyme can catalyze glucose formation. Because *M. maripaludis*, similar to other methanogens, is able to synthesize glycogen intracellularly and degrade it under starvation, the possibility has been raised regarding the production of methane from glycogen or D-glucose by methanogen itself [10]. In the absence of other annotated genes, the reversible GK activity of this bifunctional enzyme could be responsible for glucose formation in *M. maripaludis*.

To gain insights into the operation of both the direct and reverse GK reactions, we evaluated the effect of the nucleotide product. For the reverse reaction, ADP presents a strong inhibition of enzyme activity with an IC_{50} value of 80 μM when the reaction was assayed in the presence of 1 mM AMP, 6 mM $MgCl_2$ and 10 mM glucose 6*P*. On the other hand, in the direct GK reaction, AMP shows an interesting behavior; at concentrations < 5 mM, it activates glucose phosphorylating activity, whereas, at higher concentrations, it presents the expected product inhibition (not shown). Also, the complex effect of AMP is observed when acting as substrate in the reverse GK reaction, where a strong substrate inhibition effect is observed (K_i of 0.4 mM at 10 mM of glucose 6*P*). Unexpectedly, when the same experiment was performed at a glucose 6*P* concentration of 0.5 mM, a sigmoidal behavior was observed, along with an even more pronounced inhibition (Fig. 5). These results highlight the role of AMP as the key metabolite responsible for the operation of this enzyme either in the glycolytic or gluconeogenic flux direction.

The reverse catalysis for PFK activity (Table 1) showed a K_m for fructose 1,6-bisphosphate (fructose 1,6-bis*P*) similar to that obtained for fructose 6*P*, although with a k_{cat} value 36-fold lower than that determined for the direct reaction, where the efficiency of phosphatase activity is 67-fold lower than the kinase activity. The irreversibility of the kinase activity is in agreement with the presence of a gene coding a fructose 1,6-bis*P*/aldolase bifunctional enzyme in the *M. maripaludis* genome, which has been described as an enzyme that catalyzes the dephosphorylation of fructose 1,6-bis*P*, and operates only toward gluconeogenesis [17]. Although the calculated $\Delta G°$ for each of the ADP-PFK and ADP-GK reactions is a rather large negative value with a large equilibrium constant, similar to those determined for ATP [20] (Table 2), the values were obtained under standard conditions. In the cell, the mass action ratio can modified substantially the flux direction and, consequently, in the absence of information about the intracellular concentration of the substrates and products of the reactions involved, the predictive value of these constants in relation to flux direction is limited.

These results show that, besides the ADP-dependent sugar kinase from *M. jannaschii,* the enzyme from

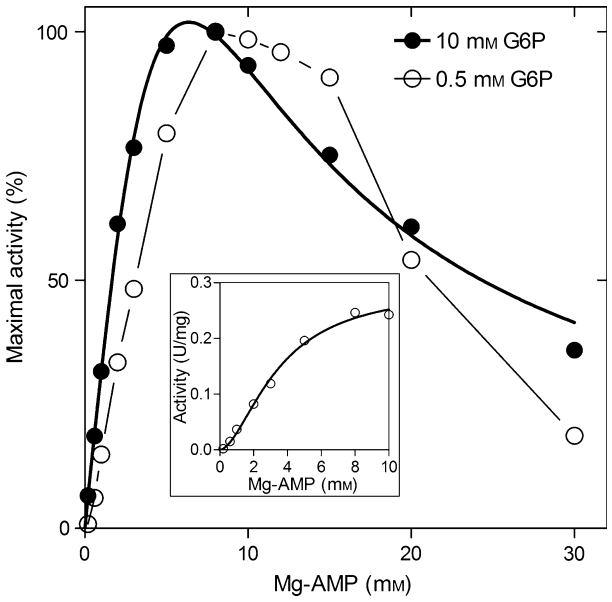

Fig. 5. Mg-AMP saturation curves for GK reverse activity. GK reverse activity in the presence of approximately 5 mM of free Mg^{2+} and different glucose 6*P* concentrations. At 10 mM of glucose 6P (G6P), a strong substrate inhibition was observed; fitting the data to a substrate inhibition equation gives a K_i of 0.4 mM. At 0.5 mM of glucose 6*P*, a more complex behavior was observed; below 10 mM of MgAMP, the saturation curve presents a sigmoidal behavior with a Hill coefficient of 1.7 (inset); over this concentration, a strong inhibition effect is observed.

Table 2. Standard free energy change of GK and PFK reactions.

Reaction	$\Delta G°$ (kJ·mol^{-1})	K_{eq} at 25 °C
ADP		
ADP-GK[a]	−19.0	2.14×10^3
ADP-PFK[a]	−16.5	7.80×10^2
ATP		
ATP-GK[b]	−16.7	8.45×10^2
ATP-PFK[b]	−14.2	3.08×10^2

[a]See supporting information (Fig. S5). [b]Jencks [20].

M. maripaludis is also able to phosphorylate glucose and fructose 6*P*. Moreover, by molecular modeling of all of the ADP-dependent family enzymes from the order *Methanococcales*, we showed that they are all bifunctional and able to phosphorylate both substrates. These results agree with the presence of only one gene of the ADP-dependent family in the genome of these organisms. By contrast, the genome of *Thermococcales* has two copies of the gene, each codifying for specific GK or PFK enzymes, which are also present in the order *Methanosarcinal* [11,15]. Future studies should investigate the relationship between the presence of only one copy of this gene and the evolutional history of the family, as well as its role in gluconeogenesis, because, according to the high conservation of the active site residues in enzymes of the order *Methanococcales*, bifunctionality is a feature shared by all its members. Moreover, the effect of the free Mg^{2+} concentration, as well as the effect of glucosamine and AMP, suggests a complex regulation of the activity of this archaeal kinase, which has not been recognized previously and could be a common feature for all the enzymes of the order *Methanococcales*.

Experimental procedures

Alignment and Bayesian inference of phylogeny

The protein BLAST web server was used to extract all of the sequences of the order *Methanococcales* present in the non-redundant protein database sequence using a PSI-BLAST algorithm with three iterations and ADP-PFK/GK from *M. jannaschii* as a template (data available up to December 2012). Multiple sequence alignment was constructed based on three-dimensional and secondary structure constraints using PROMALS3D [21] and then misaligned positions were corrected by visual inspection in MULTISEQ from VMD [22]. The Bayesian inference of phylogeny was performed using MRBAYES, version 3.1.2 [23]. For the analysis, we used Cprev as the fixed rate model, which showed a posterior probability of 1.0 in the mixed model and γ-shaped rate variation across the site with a proportion of the invariable sites. The number of generations was set to 1×10^6, and the sample frequency to 100, with two runs with four chains for each run and a temperature parameter of 0.2. The mean SD of the split frequencies was $< 1 \times 10^{-4}$. The consensus tree was calculated from 150 002 sample trees.

Expression and purification of recombinant ADP-PFK/GK homolog from *M. maripaludis*

Mm-ADP-PFK/GK cDNA (Genscript, Piscataway, NJ, USA), optimized for expression in *E. coli*, was directly cloned into the modified pET-28b vector in the restriction sites *Nde*I and *Bam*HI and its sequence was verified by DNA sequencing. This vector inserted six histidines and a cleavage site for the TEV protease into the C-terminal of the protein. *E. coli* BL21(DE3) pLysS was transformed with pET-Mmpfk/gk and grown in LB medium containing 35 μg·mL^{-1} kanamicin and 35 μg·mL^{-1} chloramphenicol at 37 °C until D_{600} of approximately 0.4 was reached. Expression of the recombinant protein was induced with 1 mM of isopropyl thio-β-D-galactoside overnight. Cell were harvested by centrifugation, suspended in binding buffer (50 mM Tris-HCl, pH 7.6, 500 mM NaCl, 20 mM imidazole and 5 mM $MgCl_2$) and disrupted by sonication. After centrifugation (18 514 ***g*** for 30 min), the soluble fraction was

loaded onto a Ni^{2+}-NTA affinity column (HisTrap HP; GE Healthcare, Little Chalfont, UK). Protein was eluted with a linear gradient between 20 and 500 mM imidazole and fractions with enzyme activity were pooled. The protein was dialyzed against 25 mM Pipes (pH 6.5) and 5 mM $MgCl_2$, and then glycerol was added to 50% v/v followed by storage at −20 °C. Enzyme purity was analyzed by SDS/PAGE stained with coomassie blue.

Determination of enzyme activity

PFK activity was assayed spectrophotometrically as described previously [24]. Briefly, enzyme preparation was mixed with reaction buffer containing 25 mM Pipes buffer (pH 6.5), 25 mM $MgCl_2$, 2 mM fructose 6*P*, 0.2 mM NADH, 20 mM ADP, 1.96 U of α-glycerophosphate dehydrogenase, 19.6 U of triosephosphateisomerase and 0.52 U of aldolase in a final volume of 0.25 mL (standard assay).

GK activity was measured spectrophotometrically by monitoring NAD^+ reduction at 340 nm, coupled with glucose 6*P* oxidation at 30 °C. A standard assay was carried out in a final volume of 0.25 mL in the presence of 25 mM Hepes (pH 7.8), 0.5 mM NAD^+, 2–5 U of glucose 6*P* dehydrogenase from *Leuconostoc mesenteroides*, 200 mM glucose, 25 mM $MgCl_2$ and 20 mM ADP (standard assay).

Reverse activities (GK and PFK) were measured by monitoring the appearance of ADP with a coupling assay containing pyruvate kinase/lactate dehydrogenase in a final volume of 0.25 mL. Briefly, enzyme preparation was mixed with reaction buffer containing 25 mM Hepes (pH 7.0), 0.4 U of pyruvate kinase, 1.2 U of lactate dehydrogenase, 0.3 mM phosphoenolpyruvate, 125 mM KCl, 0.2 mM NADH, 15 mM $MgCl_2$, 10 mM AMP and 10 mM glucose 6*P* or fructose 1,6-bis*P*.

Inhibition of the reverse GK activity by ADP was measured by monitoring glucose appearance using the glucose oxidase/peroxidase system from BioSystem (Barcelona, Spain). The assay mixture contained: 20 mM phosphate (pH 7.5), 1 mM phenol, > 2 $U \cdot mL^{-1}$ glucose oxidase, > 0.2 $U \cdot mL^{-1}$ peroxidase and 0.1 mM 4-aminopyrine. Reduction of 4-aminopyrine to quinoneimine was monitored at 500 nm.

All enzyme activities were determined at 30 °C using a UV/visible Synergy 2 spectrophotometer (BioTek, Winooski, VT, USA) and 96-well plates (model 269620; Nunc, Rochester, NY, USA). An extinction coefficient of 6.22 $mM^{-1} \cdot cm^{-1}$ for NADH and a path length correction at 1 cm was used for specific activity ($U \cdot mg^{-1}$) determination.

Reagent concentrations

Glucose and fructose 6*P* were titrated with the respective assays using ADP-dependent glucokinase from *T. litoralis* and ADP-dependent PFK from *P. horikoshii*, respectively; ADP was titrated with a GK assay using ADP-GK from *T. litoralis*, glucose 6*P* was titrated with glucose 6*P* dehydrogenase from *L. mesenteroides* and NAD^+, the titration was performed with a co-substrate concentration at least 20-fold over the compound titrated. Protein concentration was determined using the Bio-Rad protein assay (Bio-Rad, Hercules, CA, USA) and BSA Standard (Thermo Fisher Scientific Inc., Waltham, MA, USA) as a reference. Substrate titration and protein concentrations were measured in a photodiode array spectrophotometer (8453; Hewlett Packard/Agilent, Santa Clara, CA, USA).

Substrate specificity

Phosphoryl acceptor specificity of MmPFK/GK was determined by measuring the consumption of ADP in a discontinuous assay. The reaction mixture contained 25 mM Tris-HCl (pH 7.0), 20 mM $MgCl_2$, 25 mM ADP, 10 μg of MmPFK/GK and 10 mM of each sugar (17 sugars tested) in a final volume of 0.2 mL. The mixture was incubated for 15 min at 30 °C, the reaction was stopped with perchloric acid at a final concentration of 3% v/v, placed on ice for 5 min, and then the mixture was neutralized with a final concentration of $NaHCO_3$ of 0.5 M. Next, 5 μL of reaction mixture was titrated with 495 μL of ADP titration mix containing 0.8 U of pyruvate kinase, 2.4 U of lactate dehydrogenase, 0.3 mM phosphoenolpyruvate, 125 mM KCl, 25 mM Tris-HCl (pH 7.0), 5 mM $MgCl_2$ and 0.2 mM NADH at 37 °C. ADP consumption with different sugars was calculated using the reaction mixture without sugars as a reference. Activity was reported as a percentage of ADP consumption obtained with glucose in 15 min.

Activity with different nucleotides was determined by measuring PFK and GK activity as described above, substituting ADP for GDP, IDP, CDP, TDP, UDP and ATP at 10 mM for each nucleotide in the presence of 15 mM $MgCl_2$. The activity is reported as percentage of that obtained with ADP. The divalent cation preference was tested similarly; $MgCl_2$ was replaced by $CaCl_2$, $MnCl_2$, $ZnCl_2$, $NiSO_4$ and $CoSO_4$ at a concentration of 2 mM in the presence of 1 mM of ADP. Metal ion dependent catalysis was evaluated by adding 50 mM EDTA to the assay in the presence of $MgCl_2$. To discard a counterion effect, the assay was performed with $MgSO_4$, instead of $MgCl_2$, obtaining the same GK and PFK activity under both conditions (data not shown).

pH dependence

pH dependence activity was determined by measuring the PFK and GK activity spectrophotometrically as described above, substituting Pipes and Hepes buffer: pH 5.0 and 5.5 were attained with acetate/acetic acid buffer; pH 6.0, 6.6 and 7.0 were attained with Pipes buffer; pH 7.5, 8.0, 8.5 and 8.9 were attained with Tris-HCl buffer. The buffer concentration was 50 mM.

Kinetic parameters

For GK and PFK assays, kinetic parameters were determined at 30 °C, varying the concentration of substrates at the saturating co-substrate concentration. In each case, 5 mM $MgCl_2$ in excess over the nucleotide concentration (ADP or AMP) was used (approximately 5 mM free Mg^{2+} concentration). For kinetic parameters determinations at 1 mM free Mg^{2+}, a K_d of 676 μM for the Mg-ADP complex was considered; ADP protonation was neglected considering the pH of the assay. Initial velocity studies were performed twice in triplicate. Data were analyzed using nonlinear regression with GRAPHPAD PRISM, version 5.0 (GraphPad Software Inc., San Diego, CA, USA) and fitted to the Michaelis–Menten, substrate inhibition, dose-response inhibition or competitive inhibition equations.

Molecular mass determination

The molecular mass of the enzyme was determined by gel filtration on a TSK gel column G3000SWXL (7.8 mm × 30 cm) (Tosoh, Tokyo, Japan), equilibrated with column buffer (100 mM Tris-HCl, pH 7.0, 100 mM NaCl and 2 mM $MgCl_2$) and calibrated with Thyroglobuin (669 kDa), immunoglobulin G (150 kDa), myoglobin (17.6 kDa) and vitamin B_{12} (1.3 kDa).

Molecular modeling and docking

Recently, we have shown that ligands modified the major and minor domain angle in a ADP-dependent sugar kinase family member and that these conformational changes are kinetically relevant [15]. For this reason, we modeled the MmPFK/GK enzyme in the closed conformation using a modified protocol as described previously [11].

Briefly, the *P. horikoshii* PFK structure (Protein Data Bank Code: 3DRW) has a 43% identity with MmPFK/GK, although this structure is in an open conformation. The only structure in the closed conformation is GK from *Pyococcus furiosus* (Protein Data Bank Code: 1UA4), which shares only 27% sequence identity with MmPFK. Then, the 3DRW structure was split off into its large and small domains and both of them were structurally aligned with the 1UA4 structure. Next, the closed structure and the two fragments were used as templates for modeling the enzyme in the closed conformation. Fifty models were constructed with MODELLER, version 8 [25]. From these, the best 10 potential DOPE models were chosen, and quality was evaluated with PROSA2003 [26], PROCHECK [27] and VERIF3D [28] (Table S1). The same procedure was performed for each of the remaining sequences of the *Methanococcales* group, except that only 10 models were evaluated (Table S2).

Docking assays with glucose and fructose 6*P* were performed with AUTODOCKVINA, version 1.0 [29], with protonation states according to the pH values used in the kinetic experiments. The protonation state of the ionizable residues was calculated using the web server H++ [30]. After this procedure, partial charges were derivate with the Gasteiger method using AUTODOCKTOOL [31]. Residues N169 and R200 were free to move when the ligand was glucose, whereas, for fructose 6*P*, E79 and R200 were set as flexible side chains. Docking results with a lower interaction energy and the phosphoryl acceptor hydroxyl oriented towards the GXGD motif were selected because aspartic acid is considered as the catalytic base for phosphate group transfer in all ribokinase superfamily members [3]. Next, the Mg-ADP complex was mounted onto the resulting docking structures according to the procedure described by Merino *et al.* [16] and then both structures were subjected to energy minimization with NAMD, version 2.7 [32] using the CHARMM27 [33] force field. Proteins were placed in a water box, the system was neutralized with NaCl to a final concentration of 0.1 M, and 10 000 iterations were performed without restrictions.

Acknowledgements

This work was supported by Fondo Nacional de Desarrollo Cientifico y Tecnologico (Fondecyt, Chile) Grant 1110137 and CONICYT scholarship 24121448.

References

1 Tuininga JE, Verhees CH, van der Oost J, Kengen SW, Stams AJ & de Vos WM (1999) Molecular and biochemical characterization of the ADP-dependent phosphofructokinase from the hyperthermophilic archaeon *Pyrococcus furiosus*. *J Biol Chem* **274**, 21023–21028.

2 Ito S, Fushinobu S, Yoshioka I, Koga S, Matsuzawa H & Wakagi T (2001) Structural basis for the ADP-specificity of a novel glucokinase from a hyperthermophilic archaeon. *Structure* **9**, 205–214.

3 Guixé V & Merino F (2009) The ADP-dependent sugar kinase family: kinetic and evolutionary aspects. *IUBMB Life* **61**, 753–761.

4 Koga S, Yoshioka I, Sakuraba H, Takahashi M, Sakasegawa S, Shimizu S & Ohshima T (2000) Biochemical characterization, cloning, and sequencing of ADP-dependent (AMP-forming) glucokinase from two hyperthermophilic archaea, *Pyrococcus furiosus* and *Thermococcus litoralis*. *J Biochem* **128**, 1079–1085.

5 Kengen SW, Tuininga JE, de Bok FA, Stams AJ & de Vos WM (1995) Purification and characterization of a novel ADP-dependent glucokinase from the hyperthermophilic archaeon *Pyrococcus furiosus*. *J Biol Chem* **270**, 30453–30457.

6 Currie MA, Merino F, Skarina T, Wong AHY, Singer A, Brown G, Savchenko A, Caniuguir A, Guixé V, Yakunin AF *et al.* (2009) ADP-dependent

6-phosphofructokinase from *Pyrococcus horikoshii* OT3: structure determination and biochemical characterization of PH1645. *J Biol Chem* **284**, 22664–22671.
7 Ronimus RS & Morgan HW (2003) Distribution and phylogenies of enzymes of the Embden–Meyerhof–Parnas pathway from archaea and hyperthermophilic bacteria support a gluconeogenic origin of metabolism. *Archaea* **1**, 199–221.
8 Hansen T & Schönheit P (2004) ADP-dependent 6-phosphofructokinase, an extremely thermophilic, non-allosteric enzyme from the hyperthermophilic, sulfate-reducing archaeon *Archaeoglobus fulgidus* strain 7324. *Extremophiles* **8**, 29–35.
9 Verhees CH, Tuininga JE, Kengen SWM, Stams AJM, Van Der Oost J & De Vos WM (2001) ADP-dependent phosphofructokinases in mesophilic and thermophilic methanogenic archaea. *J Bacteriol* **183**, 7145–7153.
10 Sakuraba H, Yoshioka I, Koga S, Takahashi M, Kitahama Y, Satomura T, Kawakami R & Ohshima T (2002) ADP-dependent glucokinase/phosphofructokinase, a novel bifunctional enzyme from the hyperthermophilic archaeon *Methanococcus jannaschii*. *J Biol Chem* **277**, 12495–12498.
11 Merino F & Guixé V (2008) Specificity evolution of the ADP-dependent sugar kinase family: *in silico* studies of the glucokinase/phosphofructokinase bifunctional enzyme from *Methanocaldococcus jannaschii*. *FEBS J* **275**, 4033–4044.
12 Sato T & Atomi H (2011) Novel metabolic pathways in Archaea. *Curr Opin Microbiol* **14**, 307–314.
13 Say RF & Fuchs G (2010) Fructose 1,6-bisphosphate aldolase/phosphatase may be an ancestral gluconeogenic enzyme. *Nature* **464**, 1077–1081.
14 Jones WJ, Nagle DP Jr & Whitman WB (1987) Methanogens and the diversity of archaebacteria. *Microbiol Rev* **51**, 135–177.
15 Rivas-Pardo JA, Herrera-Morande A, Castro-Fernandez V, Fernandez FJ, Vega MC & Guixe V (2013) Crystal structure, SAXS and kinetic mechanism of hyperthermophilic ADP-dependent glucokinase from *Thermococcus litoralis* reveal a conserved mechanism for catalysis. *PLoS One* **8**, e66687.
16 Merino F, Rivas-Pardo JA, Caniuguir A, García I & Guixé V (2012) Catalytic and regulatory roles of divalent metal cations on the phosphoryl-transfer mechanism of ADP-dependent sugar kinases from hyperthermophilic archaea. *Biochimie* **94**, 516–524.
17 Wächtershäuser G (1988) Before enzymes and templates: theory of surface metabolism. *Microbiol Rev* **52**, 452–484.
18 König H, Nusser E & Stetter KO (1985) Glycogen in *Methanolobus* and *Methanococcus*. *FEMS Microbiol Lett* **28**, 265–269.
19 Berg IA, Kockelkorn D, Ramos-Vera WH, Say RF, Zarzycki J, Hügler M, Alber BE & Fuchs G (2010) Autotrophic carbon fixation in archaea. *Nat Rev Microbiol* **8**, 447–460.
20 Jencks WP (1976) Physical and Chemical Data. In *Handbook of Biochemistry and Molecular Biology*, 3rd edn (Fasman G, ed.), pp. 296–304. CRC Press, Cleveland, OH.
21 Pei J, Kim B-H & Grishin NV (2008) PROMALS3D: a tool for multiple protein sequence and structure alignments. *Nucleic Acids Res* **36**, 2295–2300.
22 Roberts E, Eargle J, Wright D & Luthey-Schulten Z (2006) MultiSeq: unifying sequence and structure data for evolutionary analysis. *BMC Bioinformatics* **7**, 382.
23 Ronquist F & Huelsenbeck JP (2003) MrBayes 3: Bayesian phylogenetic inference under mixed models. *Bioinformatics* **19**, 1572–1574.
24 Kengen SW, De Bok FA, Van Loo ND, Dijkema C, Stams AJ & De Vos WM (1994) Evidence for the operation of a novel Embden–Meyerhof pathway that involves ADP-dependent kinases during sugar fermentation by *Pyrococcus furiosus*. *J Biol Chem* **269**, 17537–17541.
25 Sali A & Blundell TL (1993) Comparative protein modelling by satisfaction of spatial restraints. *J Mol Biol* **234**, 779–815.
26 Sippl MJ (1993) Recognition of errors in three-dimensional structures of proteins. *Proteins Struct Funct Genet* **17**, 355–362.
27 Laskowski RA, MacArthur MW, Moss DS & Thornton JM (1993) PROCHECK: a program to check the stereochemical quality of protein structures. *J Appl Crystallogr* **26**, 283–291.
28 Bowie JU, Luthy R & Eisenberg D (1990) Fold into a known three-dimensional structure. *Science*, **253**, 164–170.
29 Trott O & Olson AJ (2009) AutoDock Vina: improving the speed and accuracy of docking with a new scoring function, efficient optimization, and multithreading. *J Comput Chem* **31**, 455–461.
30 Gordon JC, Myers JB, Folta T, Shoja V, Heath LS & Onufriev A (2005) H++: a server for estimating pKas and adding missing hydrogens to macromolecules. *Nucleic Acids Res* **33**, W368–W371.
31 Morris GM, Huey R, Lindstrom W, Sanner MF, Belew RK, Goodsell DS & Olson AJ (2009) AutoDock4 and AutoDockTools4: automated docking with selective receptor flexibility. *J Comput Chem* **30**, 2785–2791.
32 Phillips JC, Braun R, Wang W, Gumbart J, Tajkhorshid E, Villa E, Chipot C, Skeel RD, Kale L & Schulten K (2005) Scalable molecular dynamics with NAMD. *J Comput Chem* **26**, 1781–1802.
33 MacKerell AD, Bashford D, Bellott Dunbrack RL, Evanseck JD, Field MJ, Fischer S, Gao J, Guo H, Ha

S, Joseph-McCarthy D *et al*. (1998) All-atom empirical potential for molecular modeling and dynamics studies of proteins. *J Phys Chem B* **102**, 3586–3616.

Supporting information

Additional supporting information may be found in the online version of this article at the publisher's web site:

Fig. S1. SDS/PAGE of the MmPFK/GK purification.

Fig. S2. Kinetic characterization of MmPFK/GK.

Fig. S3. ADP interactions at the active site of the MmPFK/GK homology model.

Fig. S4. Comparison of the ADP-dependent sugar kinases homology models for sequences of the order *Methanococcales* with the *M. maripaludis* homology model.

Fig. S5. Estimation of standard free energy change and equilibrium constants of the ADP-GK and ADP-PFK reactions.

Table S1. Evaluation of the MmPFK/GK homology model.

Table S2. Evaluation of the ADP-PFK/GK homology models for sequences of the order *Methanococcales*.